

Observation of tancoite-like chains in a one-dimensional metal–organic polymer

A. Thirumurugan,^a Swapan K. Pati,^b Mark A. Green^c and Srinivasan Natarajan*^a

^aFramework Solids Laboratory, Chemistry and Physics of Materials Unit, Jawaharlal Nehru Centre for Advanced Scientific Research, Jakkur P.O., Bangalore 560 064, India.

E-mail: raj@jncasr.ac.in; Fax: +91-80-846-2766

^bTheoretical Sciences Unit, Jawaharlal Nehru Centre for Advanced Scientific Research, Jakkur P.O., Bangalore 560 064, India

^cThe Davy-Faraday Research Laboratory, The Royal Institution of Great Britain, 21 Albemarle Street, London, UK W1S 4BS

Received 9th September 2003, Accepted 20th October 2003

First published as an Advance Article on the web 3rd November 2003

A hydrothermal reaction of diphenic acid, NaOH, water and the corresponding lanthanide salt at a pH of ~5.5 gives rise to a new one-dimensional metal–organic coordination polymer, ${}^1\infty[\text{M}_2(\text{H}_2\text{O})_2(\text{C}_{14}\text{H}_8\text{O}_4)_3]$ (M = Nd, Dy or Y). The structure is built up from a network of distorted dodecahedral MO_8 units and the diphenate anions. The M atoms are connected through an oxygen atom, giving rise to tancoite-like chains, to which the diphenate anions are grafted completing the one-dimensional structure. Magnetic studies indicate only paramagnetic behavior in the temperature range 4–300 K for M = Dy. The compounds exhibit photoluminescence at room temperature with the main emission band at 450 nm ($\lambda_{\text{ex}} = 338$ nm).

Introduction

Synthesis of new materials with novel structures constitutes an important area of research. Inorganic–organic hybrid compounds prepared using multi-functional benzene carboxylic acids belong to this class.^{1–5} The continuing research in this area has shown that the carboxylates of lanthanides (Ln) are attractive due to the higher coordination of the Ln ions as well as for their many interesting properties.^{6–10} Though the literature abounds on the report of novel benzene carboxylates,^{3,5} those formed from specific building units or with an inorganic core are rare. In many of the benzene carboxylates, the carboxylate group locks the metal ions in position to form the clusters. Metal carboxylate clusters have been employed for the design of porous metal–organic frameworks.³ Recently, 1,4-naphthalenedicarboxylic acid has been used to form new metal–organic frameworks having cuboctahedral clusters.^{11,12} We have been interested in the use of diphenic acid for the preparation of metal–organic frameworks, especially with lanthanide ions. Interesting building units with unusual structures have been observed recently by the use of diphenic acid in the preparation of metal–organic frameworks.¹³ In continuation of the same theme, we have now discovered a new lanthanide coordination polymer, ${}^1\infty[\text{M}_2(\text{H}_2\text{O})_2(\text{C}_{14}\text{H}_8\text{O}_4)_3]$ (M = Nd, Dy or Y). More importantly, the central metal ions are locked into position by the carboxylate units to form a structure that resembles the naturally occurring mineral tancoite, $\text{LiNa}_2\text{HAl}(\text{PO}_4)_2(\text{OH})$.¹⁴ In this paper, we present the synthesis and structure of this compound along with the magnetic studies for the Dy compound.

Experimental

All the compounds have been synthesized under identical conditions employing hydrothermal methods. Typically, 0.174 g of $\text{Dy}(\text{NO}_3)_3$ and 0.252 g of diphenic acid (DPA) were dispersed in 5 ml of water. To this, 0.4 ml of NaOH (5 M solution) was added and the mixture was homogenized at room temperature for 30 min. The final mixture with composition

1 $\text{Dy}(\text{NO}_3)_3$:2 DPA:4 NaOH:556 H_2O , was sealed in a 23 ml PTFE-lined bomb and heated at 180 °C for 72 h. The resulting product contained only rod-like colorless crystals and was vacuum filtered and dried at ambient conditions. The yield of the product was ~80%. Identical composition and procedure were adapted for the neodymium and yttrium containing compounds, resulting in very high yield (>75%) of single crystalline product. The compounds were characterized by powder XRD, IR, TGA and photoluminescence studies. The powder XRD patterns were recorded on crushed single crystals in the 2θ range 5–50° using Cu-K α radiation (Rich-Seifert, 3000TT). The XRD patterns indicated that the products were new materials; the patterns were entirely consistent with the structures determined using single-crystal X-ray diffraction.

Infrared (IR) spectroscopic studies have been carried out in the mid-IR region on KBr pellets (Bruker IFS-66v). The IR spectra of all the compounds indicated characteristic sharp lines with very similar bands. Minor variations in the bands were however seen between the compounds. Observed bands/ cm^{-1} : 3639(s) and 3552(s) = $\nu_s\text{OH}$ (lattice water), 3045(w) = $\nu_{\text{as}}(\text{C-H})_{\text{aromatic}}$, 1618(s) = $\delta(\text{OH})$, $\nu_{\text{as}}(\text{C=O})$, 1521(s) = $(\text{C-C})_{\text{skeletal}}$, 1406(s) and 1442(s) = $\delta(\text{OH})$, $\delta_{\text{as}}(\text{C=O})$, 1267(w) = $\delta_s(\text{C=O})$, 1151(m) = $\delta(\text{CH}_{\text{aromatic}})_{\text{in-plane}}$, 762(s) = $\delta(\text{CH}_{\text{aromatic}})_{\text{out-of-plane}}$.

Thermogravimetric analysis (TGA) has been carried out (Mettler-Toledo, TG850) in nitrogen atmosphere (flow rate = 50 ml min^{-1}) in the temperature range 25–900 °C (heating rate = 2 °C min^{-1}). The studies indicate two weight losses. The initial weight loss of 5.3% around 200 °C corresponds to the loss of some adsorbed and the bound water (calc. 3.4%). The second weight loss of 63.45% was quite sharp at 425 °C and corresponds to the loss of the diphenate (calc. 66.29%). The total observed weight loss of 68.8% corresponds very well with the calculated weight loss of 69.6%. The calcined sample was crystalline and the powder XRD lines matches well with the corresponding lanthanide oxide. A small portion (300 mg) of the Dy sample was heated at 200 °C for 1 h to investigate whether binding of the water molecules was reversible. The powder XRD pattern recorded after the heating, reveal that the

Table 1 Crystal data and structure refinement parameters for $^1_\infty[\text{M}_2(\text{H}_2\text{O})_2(\text{C}_{14}\text{H}_8\text{O}_4)_3]$ (M = Nd, Dy and Y)

Structure parameter	Nd	Dy	Y
Empirical formula	$\text{C}_{21}\text{H}_{14}\text{NdO}_7$	$\text{C}_{21}\text{H}_{14}\text{DyO}_7$	$\text{C}_{21}\text{H}_{14}\text{YO}_7$
M_r	522.56	540.82	467.23
Crystal system	Monoclinic	Monoclinic	Monoclinic
Space group	$C2/c$ (no. 15)	$C2/c$ (no. 15)	$C2/c$ (no. 15)
$a/\text{\AA}$	20.9868(6)	20.9794(7)	20.9371(5)
$b/\text{\AA}$	21.5521(7)	21.3829(7)	21.3218(4)
$c/\text{\AA}$	8.3126(3)	8.2116(3)	8.1858(2)
$\beta/^\circ$	103.950(1)	104.089(1)	104.179(1)
$V/\text{\AA}^3$	3650.6(2)	3572.9(2)	3542.95(14)
Z	8	8	8
$D/\text{g cm}^{-3}$	1.902	2.011	1.752
μ/mm^{-1}	2.888	4.227	3.337
Total data collected	7631	7408	7296
Unique data	2624	2560	2551
Observed data	2172	2115	1807
$[I > 2\sigma(I)]$			
R_{merge}	0.0312	0.0289	0.0584
$R_1 [I > 2\sigma(I)]^a$	0.0216	0.0242	0.0378
$wR_2 [I > 2\sigma(I)]^b$	0.0524	0.0601	0.0702
R_1 (all data) ^a	0.0284	0.0315	0.0709
wR_2 (all data) ^b	0.0546	0.0631	0.0816

^a $R_1 = \Sigma||F_o| - |F_c||/\Sigma|F_o|$. ^b $wR_2 = \{\Sigma[w(F_o^2 - F_c^2)^2]/\Sigma[w(F_o^2)^2]\}^{1/2}$; $w = 1/[\sigma^2(F_o)^2 + (aP)^2 + bP]$, $P = [\max(F_o^2, 0) + 2(F_c^2)]/3$, where $a = 0.0284$ and $b = 0.0$ for Nd, $a = 0.0307$ and $b = 5.7019$ for Dy, and $a = 0.0245$ and $b = 3.3433$ for Y.

sample is crystalline with additional uncharacterized lines, indicating the possible collapse of the structure with the loss of bonded water.

A suitable single crystal of each compound was carefully selected under a polarizing microscope and glued to a thin glass fiber. Crystal structure determination by X-ray diffraction was performed on a Siemens's Smart-CCD diffractometer equipped with a normal focus, 2.4 kW sealed tube X-ray source (Mo-K α radiation, $\lambda = 0.71073$ Å) operating at 40 kV and 40 mA. An empirical absorption correction based on symmetry equivalent reflections was applied using the SADABS program.¹⁵ The structure was solved and refined using the SHELXTL-PLUS suite of program.¹⁶ All the hydrogen atoms of the carboxylic acids and the bound water molecules were located in the difference Fourier maps. For the final refinement the hydrogen atoms on the carboxylic acid were placed geometrically and held in the riding mode. Final refinement included atomic positions for all the atoms, anisotropic thermal parameters for all the non-hydrogen atoms and isotropic thermal parameters for all the hydrogen atoms. Full-matrix least-squares refinement against $|F^2|$ was carried out using the SHELXTL-PLUS¹⁶ suite of programs. Details of the structure solution and final refinements for the compounds $^1_\infty[\text{M}_2(\text{H}_2\text{O})_2(\text{C}_{14}\text{H}_8\text{O}_4)_3]$ (M = Nd, Dy and Y) are given in Table 1 and the selected bond distances in Table 2.

CCDC reference numbers 218557–218559.

See <http://www.rsc.org/suppdata/jm/b3/b310778g/> for crystallographic data in CIF or other electronic format.

Results and discussion

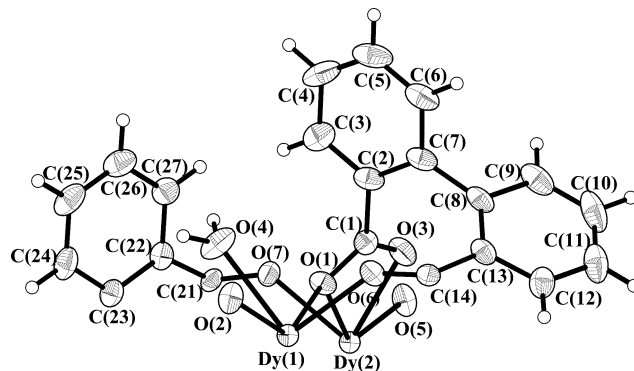
All the three compounds are isostructural and for the description of the structure we consider the dysprosium compound. The asymmetric unit, shown in Fig. 1, consists of two Dy atoms, each of which lies on the crystallographic two-fold axis with a site-occupancy (SOF) of 0.5. The Dy atoms are coordinated to eight nearest-neighbor oxygen atoms and have a distorted dodecahedral arrangement. The oxygen atoms, in turn, are connected to the carbon atoms of the carboxylate group, except O(4), which is a terminal water molecule. The Dy–O distances are in the range 2.267(3)–2.582(3) Å (av. 2.393 Å) and O–Dy–O bond angles are in the range 52.30(10)–148.79(10) $^\circ$ (av. 101.8 $^\circ$). There are two

Table 2 Selected bond distances (Å) in $^1_\infty[\text{M}_2(\text{H}_2\text{O})_2(\text{C}_{14}\text{H}_8\text{O}_4)_3]$ (M = Nd, Dy and Y)

	Nd	Dy	Y
M(1)–O(1)	2.342(2)	2.267(3)	2.243(3)
M(1)–O(1)#1	2.342(2)	2.267(3)	2.243(3)
M(1)–O(2)	2.508(2)	2.435(3)	2.418(3)
M(1)–O(2)#1	2.508(2)	2.435(3)	2.418(3)
M(1)–O(3)	2.502(2)	2.438(3)	2.418(3)
M(1)–O(3)#1	2.502(2)	2.438(3)	2.418(3)
M(1)–O(4)	2.561(3)	2.464(3)	2.434(4)
M(1)–O(4)#1	2.561(3)	2.464(3)	2.434(4)
M(2)–O(1)	2.635(2)	2.582(3)	2.572(3)
M(2)–O(1)#2	2.635(2)	2.582(3)	2.572(3)
M(2)–O(5)	2.362(2)	2.276(3)	2.269(3)
M(2)–O(5)#2	2.362(2)	2.276(3)	2.269(3)
M(2)–O(6)	2.369(2)	2.289(3)	2.363(3)
M(2)–O(6)#2	2.369(2)	2.289(3)	2.363(3)
M(2)–O(7)	2.459(2)	2.387(3)	2.254(3)
M(2)–O(7)#2	2.459(2)	2.387(3)	2.254(3)
O(1)–C(14)	1.259(4)	1.268(5)	1.270(5)
O(2)–C(21)#3	1.246(4)	1.252(5)	1.265(5)
O(3)–C(1)	1.278(4)	1.281(5)	1.284(5)
O(4)–H(51)	0.943(10)	0.946(11)	0.943(10)
O(4)–H(52)	0.942(10)	0.945(10)	0.943(10)
O(5)–C(14)#4	1.256(4)	1.255(5)	1.265(5)
O(6)–C(1)	1.245(4)	1.244(5)	1.250(5)
O(7)–C(21)	1.258(4)	1.264(5)	1.255(5)

Symmetry transformations used to generate equivalent atoms: #1 $-x, y, -z + 1/2$; #2 $-x, y, -z - 1/2$; #3 $x, y, z + 1$; #4 $x, y, z - 1$.

types of diphenates present in the structure; acid-1 is formed by the carbon atoms C(1)–C(14) with C(1) and C(14) being the terminal carboxylate groups, while acid-2 is formed by the carbon atoms C(21)–C(28) with the C(23)–C(23*) bond positioned on a two-fold axis and C(21) as the carboxylate group. The torsion angles between the two benzene rings for acid-1 are 115.5 $^\circ$ [C(2), C(7), C(8) and C(9)] and 118.8 $^\circ$ [C(13), C(8), C(7) and C(6)] and for acid-2 are 56.56 $^\circ$ [C(22), C(23), C(23) and C(22)] and 58.21 $^\circ$ [C(24), C(23), C(23) and C(24)], respectively. The angle between the two phenyl rings of the diphenic acid, calculated from the mean plane, is 69.18 $^\circ$ for acid-1 and 56.88 $^\circ$ for acid-2. Though both the acids are connected to three Dy³⁺ ions, the connectivity between the acid and the Dy ions are different (Fig. 2). While acid-1 is connected to two Dy(2) and one Dy(1) through one bis-bidendate and two monodendate connections, acid-2 is connected to two Dy(1) and one Dy(2) through essentially monodendate connectivity. The C(1) carboxylate groups of acid-1 has bis-bidendate connectivity with Dy(2) and also connects Dy(1) through O(1), which shows three-coordination (two Dy and one C). The Dy atoms also show differences in their connectivity with the diphenic carboxylates. Thus, Dy(1) is connected to two acid-1 and two acid-2 units and possesses two terminal water molecules [O(4)], while Dy(2) is connected to four acid-1 and

**Fig. 1** ORTEP plot¹⁷ showing the connectivity in $^1_\infty[\text{Dy}_2(\text{H}_2\text{O})_2(\text{C}_{14}\text{H}_8\text{O}_4)_3]$. Thermal ellipsoids are given at 50% probability.

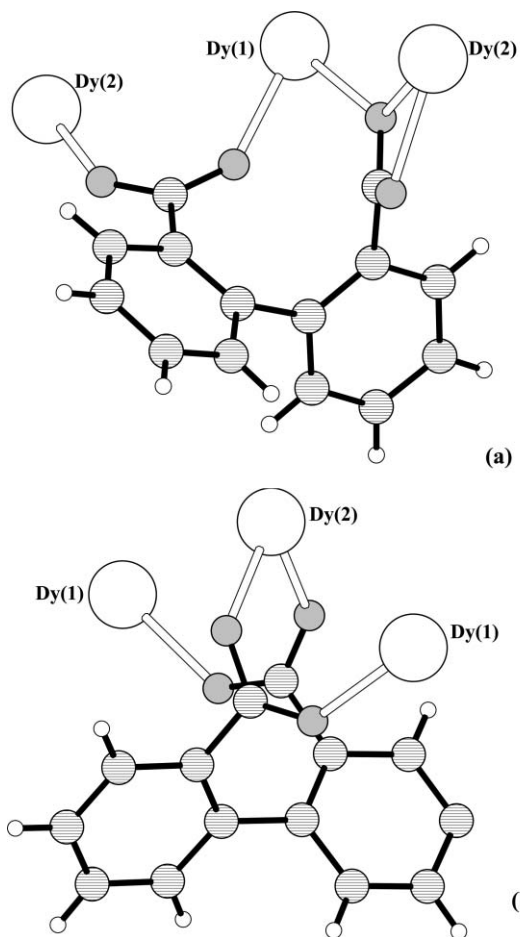


Fig. 2 Views showing the connectivity between the diphenate anion and Dy: (a) acid-1 and (b) acid-2.

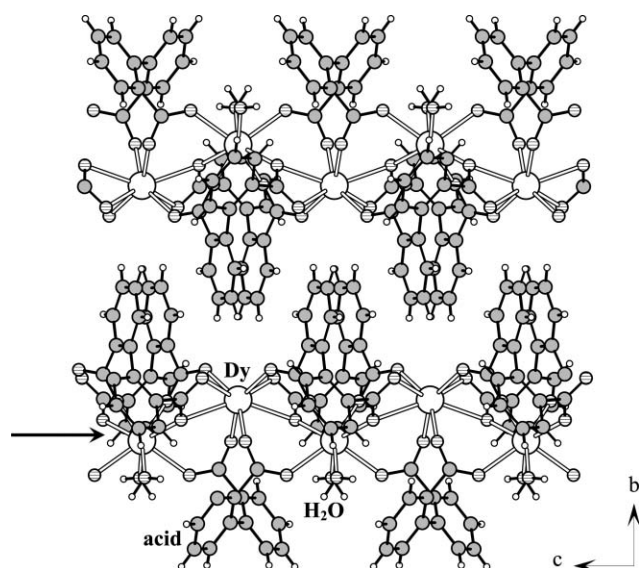


Fig. 3 The structure of ${}^1_\infty[\text{Dy}_2(\text{H}_2\text{O})_2(\text{C}_{14}\text{H}_8\text{O}_4)_3]$ in the bc plane. The arrow indicates the tancoite chain (shown as open bonds).

one acid-2 units. The various structural parameters observed in ${}^1_\infty[\text{M}_2(\text{H}_2\text{O})_2(\text{C}_{14}\text{H}_8\text{O}_4)_3]$ ($\text{M} = \text{Nd}, \text{Dy}$ and Y), are as expected for this bonding and agree with those reported in the literature for benzene carboxylate compounds.^{6–10}

The structures of the title compounds consist of a network of distorted LnO_8 dodecahedra and the diphenate anions. The Ln atoms are connected together through a central oxygen, O(1), which has three-coordination, forming one-dimensional

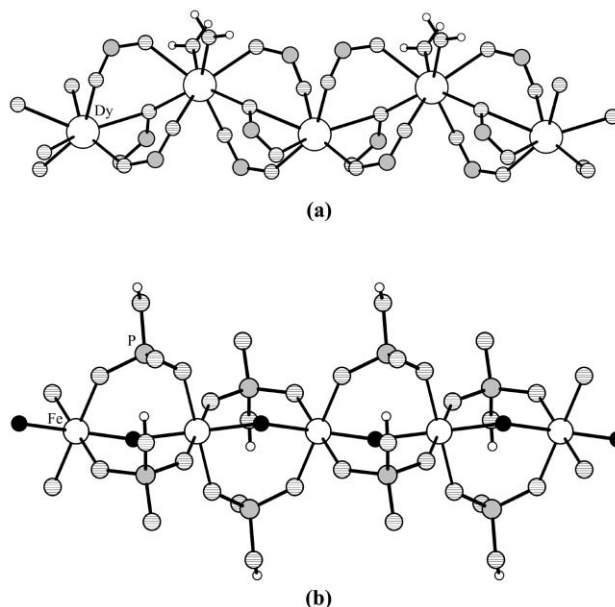


Fig. 4 (a) The tancoite chain core observed in ${}^1_\infty[\text{Dy}_2(\text{H}_2\text{O})_2(\text{C}_{14}\text{H}_8\text{O}_4)_3]$. (b) The tancoite chain observed in the iron phosphate, $[\text{NH}_3\text{CH}_2\text{CH}_2\text{CH}(\text{NH}_3)\text{CH}_2\text{CH}_3]^{2+} \cdot [\text{FeF}(\text{HPO}_4)_2]^{2-}$.

infinite $\text{Ln}-\text{O}-\text{Ln}$ chains. The carboxylic acid groups are connected to the Ln ions completing the one-dimensional structure. The view of the structure in the bc plane is shown in Fig. 3. As can be noted, the connectivity appears to be such that the carboxylates are grafted on to the central $\text{Ln}-\text{O}-\text{Ln}$ core. The diphenic units hang from the central chain into the inter-chain spaces. Looking down the chain axis (ab plane), the structure reveals that there are no direct $\pi\cdots\pi$ interactions between the diphenic groups of adjacent chains.

What is most remarkable about the present structures is the striking similarity to the naturally occurring mineral tancoite. Tancoite chains, generally, have the composition, $[\text{M}(\text{TO}_4)_2\text{L}]_n$ (M and T are cations of different coordination, usually octahedral and tetrahedral, $\text{L} =$ anionic ligand, *e.g.*, O^{2-} , OH^- or F^-).¹⁴ Tancoite-like structures have been observed in many one-dimensional phosphates,¹⁸ and recently Atfield and co-workers have isolated an aluminum diphosphonate possessing the tancoite structure.¹⁹ In the present compounds, the tancoite structure can be generated as follows: $\text{M} = \text{Ln}$ ions, $\text{T} =$ the C atoms of the carboxylate unit and $\text{L} =$ three-coordinated oxygen atoms. The observation of tancoite chains in a carboxylic acid is, indeed, noteworthy. In Fig. 4, the tancoite core observed in the present compounds is compared with that observed in iron phosphates. The present structures are somewhat similar to the ytterbium naphthalenedicarboxylate, $[\text{Yb}_2(\text{NDC})_3(\text{H}_2\text{O}) \cdot (\text{H}_2\text{O})_2]_n$ (CUMOF-9), reported recently.¹² In CUMOF-9, all the Yb atoms are connected only through the carboxylate units and there are no $\text{Yb}-\text{O}-\text{Yb}$ bridges. In the present compounds the presence of the three-coordinated oxygen atoms gives rise to infinite one-dimensional $\text{Ln}-\text{O}-\text{Ln}$ bridges.

In order to evaluate the possible effects of the tancoite-type connectivity on the magnetic properties, we have performed magnetic investigations on the Dy compound using a SQUID magnetometer. Most of the tancoite related compounds, formed using magnetic ions such as Fe, generally exhibit anti-ferromagnetic behavior.²⁰ The results of the magnetic studies on the Dy compound are presented in Fig. 5. The magnetic susceptibility indicates only paramagnetic behavior up to the lowest temperature investigated. The variation of $1/\chi$ vs. temperature is shown as an inset in Fig. 5. The dotted line is the Curie–Weiss fit to the data with $\theta_p = -1.5$ K. Assuming the crystal field splitting to be small, the 9 electrons in the

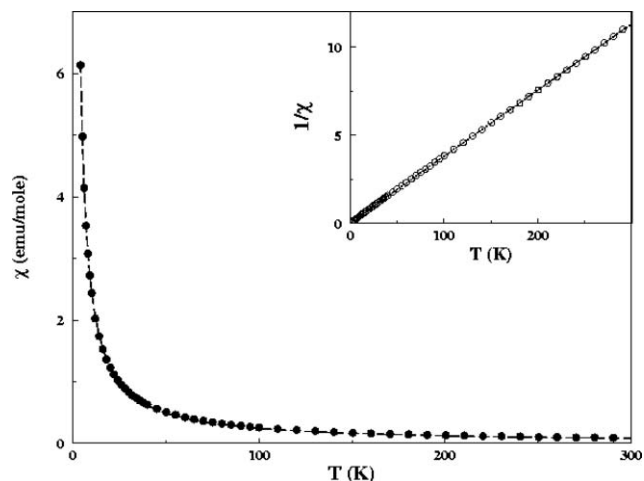


Fig. 5 The variation of magnetic susceptibility as a function of temperature for $[\text{Dy}_2(\text{H}_2\text{O})_2(\text{C}_{14}\text{H}_8\text{O}_4)_3]$. The inset shows the $1/\chi$ vs. T plot. Dotted lines represent the fit to the experimental data using a dimer model (see text).

4f-orbitals of Dy^{3+} ion would give rise to a spin of $S = 5/2$. Since the θ_p value is quite small, we have employed a dimer model with two $S = 5/2$ spins. The magnetic energy levels can be written as $E_S = \Sigma_S J/2[S(S+1) - 17.5]$ with S values ranging from 0 to 5. The magnetic susceptibility for the $S = 5/2$ dimer can be written as $\chi_{\text{dimer}} = g^2 \mu_B^2 / K_B T [\Sigma_S \{S(S+1) \exp(E_S/k_B T)\} / \Sigma_S \exp(E_S/k_B T)]$, $S = 0, 1, \dots, 5$. In Fig. 5, we have fitted this dimer susceptibility with the experimental χ_m , varying the exchange constant, J , and the Lande factor, g . The dimer model appears to be quite good over all the temperature range investigated, with $g = 2.7$ and $J = -1.2$ K, as expected. The lowest magnetic gap is 1.2 K ($-J$) from the dimer model and the small J value indicates that the Dy magnetic moments are very weakly coupled. It is to be noted that the Lande factor, g , here is the spin-only value.

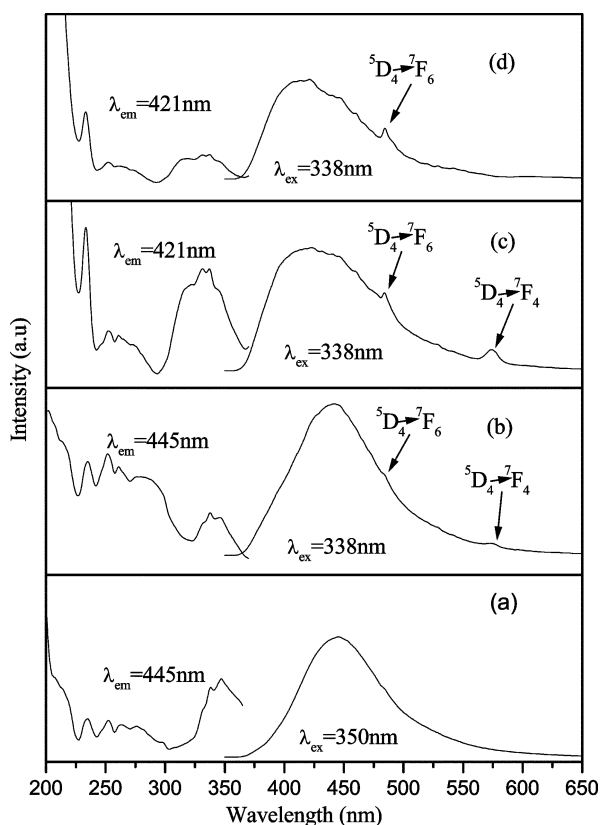


Fig. 6 Solid-state photoluminescence spectra of (a) DPA, (b) Y, (c) Dy and (d) Nd compounds at room temperature.

From the above, it appears that the net interaction $\Sigma J_{\text{Dy-Dy}}$ between Dy moments are so small that each Dy spin can be assumed to be free even at very low temperature. This is perfectly justified since the dimer model with very small superexchange value fits fairly well with the magnetic data even at the lowest temperature (4 K). Although the Dy spin is moderately large ($S = 5/2$) and can be assumed to be almost classical, the dipolar coupling is quite small due to the large nearest neighbor Dy–Dy spacing (~ 4.4 Å). In fact, with a $S = 5/2$ magnetic dipole, the dipolar coupling turns out to be little smaller than the magnetic exchange coupling. Since the energy scales are quite small, it is difficult to rule out the dominant term, both being of the order or smaller than 1 K. However, with negligible super-exchange interactions, the paramagnetic nature of the Dy spins is well expected down to temperatures of the order of the exchange energy scale. Thus, it appears that only at very low temperature that the magnetic dipole or the spin–orbit coupling effects would be important. However, this effect requires knowledge about the strength of Coulombic terms, which in turn depend on the degree of delocalization of both the 4f orbitals and the electrons in them.

The optical properties of the benzene carboxylates have been investigated since they involve the 4f orbitals, which are generally well shielded from their chemical environments by $5s^2$ and $5p^6$ electrons. The f–f transitions are parity forbidden, which leads to unfavorable excitation of the lanthanide ions. Diffuse reflectance UV-vis spectra for the DPA, and the as-synthesized compounds show similar absorption features. These are essentially two bands for the acid and the polymers, the lower wavelength band of the polymers appearing to have higher intensity compared to the acid. This, probably, indicates that there is charge-transfer from the O atoms of the carboxylates to the 4f orbitals of the lanthanide ions.

Photoluminescence studies, carried out in the solid state at room temperature, show that both the acid and the polymers show photoluminescence (Fig. 6). The main emission peak for the acid and the polymer is located at the same position, at ~ 450 nm. While the emission band for the acid may be attributable to the $\pi^* \rightarrow n$ transitions, that of the coordination polymer is attributed to the intra-ligand fluorescent emission. In addition, the polymers also exhibit additional emission bands when excited at 338 nm. These bands correspond to some of the expected $^5\text{D}_4 \rightarrow ^7\text{F}_n$ transitions.

In summary, the synthesis, structure and magnetic studies of a series of new one-dimensional coordination polymers of lanthanide diphenates has been accomplished. Optical studies indicate that the compounds show good photoluminescence behavior. While the presence of the tancoite-like structure is noteworthy, the absence of magnetic ordering is intriguing.

Acknowledgements

S. N. thanks the Department of Science and Technology (DST), Government of India for the award of a research grant and A. T. thanks the Council of Scientific and Industrial Research (CSIR), Government of India for the award of a research fellowship. The authors also thank the referees for their helpful suggestions.

References

- 1 S. Batten and R. Robson, *Angew. Chem., Int. Ed.*, 1998, **37**, 1460.
- 2 J. Hargman, D. Hargman and J. Zubieta, *Angew. Chem., Int. Ed.*, 1999, **38**, 2638.
- 3 M. Eddaoudi, D. Moler, H. Li, B. Chen, T. M. Reineke, M. O'Keefe and O. M. Yaghi, *Acc. Chem. Res.*, 2001, **34**, 319.
- 4 B. Moulton and M. Zaworotko, *Chem. Rev.*, 2001, **101**, 1629.
- 5 C. N. R. Rao, S. Natarajan and R. Vaidyanathan, *Angew. Chem., Int. Ed.*, 2003, in press.
- 6 R. Cao, D. Sun, Y. Liang, M. Hong, K. Tatsumi and Q. Shi, *Inorg. Chem.*, 2002, **41**, 2087.

- 7 T. M. Reineke, M. Eddaoudi, M. O'Keefe and O. M. Yaghi, *J. Am. Chem. Soc.*, 1999, **121**, 1651.
- 8 V. Kiritsis, A. Michaelides, S. Skoulika, S. Golhen and L. Quahab, *Inorg. Chem.*, 1998, **37**, 3407.
- 9 L. Pan, K. M. Adams, H. E. Hernandez, X. Wang, C. Zheng, Y. Hattori and K. Kaneko, *J. Am. Chem. Soc.*, 2003, **125**, 3062.
- 10 R. Wang, H. Liu, M. D. Carducci, T. Jin, C. Zheng and Z. Zheng, *Inorg. Chem.*, 2001, **40**, 2743.
- 11 D. T. Vodak, M. E. Braun, J. Kim, M. Eddaoudi and O. M. Yaghi, *Chem. Commun.*, 2001, 2534.
- 12 F. A. A. Paz and J. Klinowski, *Chem. Commun.*, 2003, 1484.
- 13 R. Wang, M. Hong, J. Luo, R. Cao and J. Weng, *Chem. Commun.*, 2003, 1018.
- 14 F. C. Hawthorne, *Acta Crystallogr., Sect. B*, 1994, **50**, 481, and references therein.
- 15 G. M. Sheldrick, *SADABS Siemens Area Detector Absorption Correction Program*, University of Göttingen, Göttingen, Germany, 1994.
- 16 G. M. Sheldrick, *SHELXTL-PLUS Program for Crystal Structure Solution and Refinement*, University of Göttingen, Göttingen, Germany, 1997.
- 17 C. K. Johnson, *ORTEP-II: A FORTRAN Thermal Ellipsoid Plot Program for Crystal Structure Illustrations*, Report ORNL-5138, Oak Ridge National Laboratory, Oak Ridge, TN, USA, 1976.
- 18 S. Mahesh, M. A. Green and S. Natarajan, *J. Solid State Chem.*, 2002, **165**, 334, and references therein.
- 19 H. G. Harvey, S. J. Teat, C. C. Tang, L. M. Cranswick and M. P. Attfield, *Inorg. Chem.*, 2003, **42**, 2428.
- 20 M. Cavellec, D. Riou, J. M. Greneche and G. Ferey, *Inorg. Chem.*, 1997, **36**, 2187, and references therein.